Applied Surface Science 695 (2025) 162790

Contents lists available at ScienceDirect

Applied Surface Science

journal homepage: www.elsevier.com/locate/apsusc

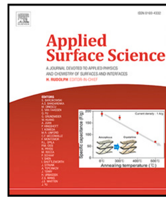

Full length article

Effects of ultra-high vacuum treatments on n-type Si contact resistivity

Mikko Miettinen [a,*], Esa Vuorinen [a], Juha-Pekka Lehtiö [a], Zahra Jahanshah Rad [a], Risto Punkkinen [a], Mikhail Kuzmin [a], Jarno Järvinen [a], Ville Vähänissi [b], Pekka Laukkanen [a,*], Hele Savin [b], Kalevi Kokko [a]

[a] Department of Physics and Astronomy, University of Turku, Turku, FI-20014, Finland
[b] Department of Electronics and Nanoengineering, Aalto University, Espoo, FI-02150, Finland

ARTICLE INFO

Keywords:
n-Si
UHV
TLM
Contact resistivity

ABSTRACT

Most electronic and photonic devices include ohmic metal–semiconductor junction(s), of which contact resistivity needs to be minimized for best efficiency of the devices. Interface defects in the junction usually degrade the junction's performance, thus cleaning and passivation of semiconductor surface is crucial during contact fabrication. For silicon devices the RCA (Radio Corporation of America) cleaning has been the most known method. Here we have addressed the question whether it is still possible to develop Si surface treatments to decrease the contact resistivity. We have combined wet chemistry and ultra-high vacuum (UHV) heating for two cases: low and highly phosphorus-doped n-type Si. As compared to silicon surfaces treated only with wet chemistry, the contact resistivity is lowered when (i) lowly doped n-Si is rapidly heated at temperature around 1200 °C in UHV followed by hydrofluoric (HF) acid dip before Ni sputtering; (ii) p-Si substrate with highly n-type surface is first immersed in HF, then UHV heated at 400 °C followed by immersion to HF. Our results show that the final HF dip decreases surface oxide formation in air during sample transfer to the metal deposition, and that surface phosphorus concentration decreases at highly doped n-Si surfaces during elevated temperature UHV heating.

1. Introduction

A clean and crystalline semiconductor surface has typically a strong tendency towards reconstructions, e.g., Si(100) (2 × 1) + (1 × 2), which means that the surface lattice has changed as compared to the corresponding atomic plane in the bulk crystal. Furthermore, changes in the atomic structure cause the changes in the valence electron-level distribution, like the dangling-bond induced levels in the bulk band-gap area. It is well known that it is challenging to prepare and keep a clean and crystalline semiconductor surface [1–4]. The common wet-chemical cleaning methods for a semiconductor surface remove most oxide and carbon contaminants, but the surface structure is still far from the crystalline, long-range ordered surface after the wet chemistry. In other words, the topmost surface has typically a disordered or amorphous structure after a wet chemical cleaning. It is also very difficult or impossible to avoid the incorporation of oxygen and carbon atoms into the cleaned surfaces during device fabrication. Thus, interfaces of semiconductor crystals are often a weak part of devices. The passivation of semiconductor surface defects has been indeed investigated and developed for devices for several decades [5–12].

Semiconductor industry has used the alloyed silicide contacts (e.g., Ni_xSi_y and Pt_xSi_y) in various silicon devices. Nickel silicide phases and their effects on the contact resistance belong to the most studied silicide properties [13–16]. The benefits of NiSi monosilicides include a low processing temperature (typically below 500 °C), reduced required amount of Si for silicide formation and applicability also for the SiGe system, while the disadvantages include a relatively low thermal stability against post-heating induced changes, e.g., towards a high-resistivity $NiSi_2$ phase. Silicon defects such as vacancies and impurities typically enhance the heating-induced degradation of the silicide contacts. Contact areas containing NiSi have been found to include defect-induced energy levels 0.5 eV below the conduction band minimum and 0.2 eV above the valence band maximum of the Si band gap, which can further cause the carrier losses via surface recombination [15,16]. Surface areas of Si crystals have an influence on the silicide formation and durability because semiconductor surfaces are often the most defect-rich part of a semiconductor crystal. The surface properties like smoothness, degree of crystallinity, and oxygen and carbon impurity concentrations readily affect the resulting metal contact performance.

* Corresponding authors.
E-mail addresses: miolmi@utu.fi (M. Miettinen), peklau@utu.fi (P. Laukkanen).

https://doi.org/10.1016/j.apsusc.2025.162790
Received 25 November 2024; Received in revised form 31 January 2025; Accepted 22 February 2025
Available online 4 March 2025
0169-4332/© 2025 The Authors. Published by Elsevier B.V. This is an open access article under the CC BY license (http://creativecommons.org/licenses/by/4.0/).

The RCA (the Radio Corporation of America) chemical procedure is one of the most common methods for cleaning Si device surfaces. Since this is so common, there is little recent comparison whether the RCA-based surface preparation can be further developed from the contact fabrication viewpoint. However, it is relevant to optimize every process step when the components integration density and power efficiency are increased. For example, ultra-high vacuum (UHV) technique, which is expected to provide a very clean environment for surface preparations, is considered to be a complex method for industry. On the other hand, UHV environment has enabled preparation of atomically smooth and crystalline surface for many semiconductors, and UHV-based instruments such molecular beam epitaxy, UHV chemical vapour deposition (CVD) and rapid thermal annealing (RTA) belong to the available arsenal of commercial tools. However, it is still unclear how UHV treatments can be integrated into the contact fabrication process in an optimized way.

In this paper we have investigated this issue using two types of silicon: lowly bulk doped n-Si and p-Si substrate with highly doped n^+ surface. We use two wet chemical methods, RCA and hydrofluoric acid (HF) dip, and UHV heatings to treat the surfaces before contact manufacturing. Our results show that despite formation of PtSi and NiSi silicides, the resistivity can be altered by combining chemical and UHV heating in proper way.

2. Experimental methods

2.1. Sample preparation

$6 \times 12\ \mathrm{mm}^2$ sample pieces were cut from two types of wafers: n-type Si (P-doped, resistivity 3–9 cm, doping concentration approximately $5 \times 10^{14}\ \mathrm{cm}^{-3} - 1 \times 10^{15}\ \mathrm{cm}^{-3}$) and p-type Si with n^+ doping on both sides (P-doped using $POCl_3$ gas diffusion, sheet resistance 115 /sq). n^+-Si doping profile is similar to samples described in article by Pasanen et al. [17]. Doping concentration for n-Si was approximated using literature [18]. Treatments used were RCA cleaning, 5 s dip to 5% aqueous HF solution, UHV heating or a combination of these. Before RCA the surface was cleaned from organic residue with individual ultrasonic baths using acetone (C_3H_6O), methanol (CH_3OH) and 2-propanol (C_3H_8O) for 3 min each. Then the sample was inserted to 80 °C solution consisting of H_2SO_4 (95%–97%):H_2O_2 (30%) (3:1) for 15 min. After this sample was immersed to 80 °C SC-1 solution NH_4OH (28%–30%):H_2O_2 (30%):H_2O (1:1:5) for 15 min following immersion to 80 °C SC-2 HCl (37%):H_2O_2 (30%):H_2O (1:1:6). Between each step the sample was rinsed thoroughly with de-ionized water (DIW) and blow-dried with N_2. After RCA the sample was dipped into 5% HF solution for five seconds. HF was used to remove the surface oxide and to create a hydrogen terminated surface to prevent surface oxidation during transfer to metal deposition facilities. All samples dipped to HF were DIW rinsed and dried unless stated otherwise.

Temperatures in UHV heating ranged from 400 °C to 1200 °C. All heat treatments were done in a UHV multi-chamber consisting of loading chamber, preparation chamber and analysis chamber. Heatings were done in analysis chamber with base pressure less than 10^{-9} mbar. For heatings under 800 °C , a resistive heater positioned beneath the sample in UHV chamber was used. For temperatures of 800 °C and over a direct current was conducted through the sample piece. Heating time depended on chosen temperature: for 400 °C 30 min, for 800 °C 5 min and for 1200 °C 5 s at the time. 1200 °C heating is later referred as flash heating, and it was the only heating temperature which was used as an individual cleaning method. Prior to heating to 1200 °C the sample was out-gassed at 600 °C overnight in UHV to prevent excess pressure increase in the chamber during flash cycle. After degassing, five cycles of flashing were done by quickly ramping the temperature up to 1200 °C, kept there for 5 s and then cooling back down to 600 °C. With other temperatures the sample was heated directly to target temperature and cooled directly to room temperature. Temperatures were observed using pyrometer measuring through a vacuum chamber view-port using emissivity of 0.63.

For contact metal deposition sputtering device Bal-Tec Med 020 was used. Temperature during sputtering was 100 °C in order prevent possible defects resulted from humidity. Since the device was in separate location, all samples were exposed to air for durations in approximately 23 min. This was also the reason why there is surface characterization done after 23 min of air exposure. Pt was used for n-Si and both Pt and Ni for n^+-Si. Pt layer thickness was 270 nm and Ni layer thickness 100 nm. Most of the contacts were patterned using standard lithography with positive photoresist with baking temperatures being 115 °C at the highest. Excess metal was etched using boiling HCl (37%):HNO_3 (65%) (1:1) for Pt and room temperature HCl (37%):H_2O (1:2) for Ni. One test sample was patterned with lift-off lithography using Kloé Dilase 250 laser writer. Resulted pattern consisted of four rows of rectangular contacts with dimensions of 300 ţm × 600 ţm (width × length). Distance between first contact columns was 300 ţm, and the distance increased by 100 ţm after each column onwards (1st–2nd 300 ţm, 2nd–3rd 400 ţm, 3rd–4th 500 ţm...). Post heatings for contacts were done in same UHV multichamber described earlier at 350 °C for 1 h.

2.2. Surface and electrical characterization

For surface characterization in-situ x-ray photoelectron spectroscopy (XPS), low-energy electron diffraction (LEED) and scanning tunneling microscopy/spectroscopy (STM/STS) as well as ex-situ XPS were used. In-situ XPS featured a non-monochromatized Mg K-α x-ray source with spot size of 3-4 mm without charge compensation, and was used to estimate the surface composition during UHV processing. Ex-situ XPS used was Thermo Scientific Nexsa system with monochromatized Al K-α x-ray source with charge compensation and adjustable spot size. Ex-situ XPS was used to measure samples mimicking air exposure of the contact samples just before metal deposition and check surface composition after metal deposition. XPS spectra from silicon 2p were normalized to find shape differences in peaks. Due to aligning the Si 2p peaks, spectra were calibrated using Si 2p binding energy value [19]. Presented spectra are collected with spot size of 150 ţm and pass energy of 30 eV. LEED was used to define surface reconstruction and STM for imaging crystallinity and possible contamination islands on the surface. Separate samples were from XPS were prepared for LEED and STM for studying surface conditions before metal deposition. All in-situ measurement devices were in the same UHV chamber where the heatings were made.

Electrical characterization was done using Rucker & Kolls 666 4-point needle probing stage with HP4145B semiconductor parameter analyzer utilizing transmission length measurement (TLM) method [20]. All samples were measured using at least two different contact rows to ensure uniformity of the contact resistivities across the sample. Current–voltage (IV) characteristics was measured from each row using at least three contact pairs, preferably four. Presented contact resistivity values are average values calculated based on multiple measurements from same sample using different contact rows, and examples of distance-resistance plots can be seen in Supplementary Fig. S1.

3. Results

3.1. Surface characterization

For low doped n-Si the most interesting treatment was a UHV heating at 1200 °C (later referred as flash or flash heating, see 2.1) followed by HF dip. As the time used to transfer the sample from UHV or chemical solution to the sputter was 23 min, that was used as mimic sample air exposure time as well. Chemical composition of flashed sample with HF dip was compared with a sample with only flash heating to see the effect of HF to the surface chemistry.

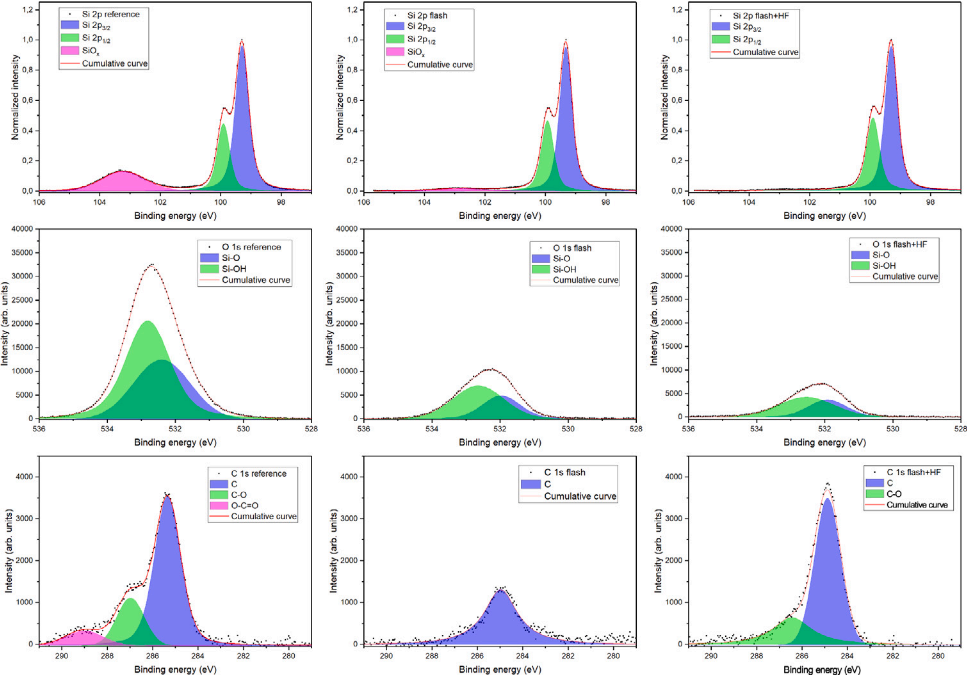

Fig. 1. Si 2p (top row), O 1s (middle row) and C 1s (bottom row) XPS spectra from n-Si in three conditions: reference (left column), after flash heating followed by 23 min air exposure (middle column) and after combination of flash heating and HF dip followed by 23 min air exposure (right column). The amount of oxygen is clearly reduced after the treatments, and SiO_2 component is either very small (flash) or completely disappeared (flash+HF). The amount of carbon is reduced by flash heating but treating the surface with HF after it clearly has made the surface attractive for carbon.

Fig. 1 shows the Si 2p, O 1s and C 1s spectra from reference sample without any treatment, a sample flashed and exposed to air for 23 min, and a sample flashed and HF dipped exposed to air for 23 min. In reference sample, the Si 2p spectrum shows clear silicon native oxide component at 103.5 eV. Oxygen and carbon signals are also strong. After flash heating, despite the air exposure, only very marginal signal from SiO_2 component is visible. O 1s signal is clear, but still significantly smaller than in reference sample. Also, carbon concentration had decreased. In-situ XPS right after flash proved that all carbon and oxygen unrelated to equipment was removed (not shown). This suggests that during 23 min of air exposure, unprotected surface reacts with air, but the growth of full native oxide is not immediate, and amount of carbon and oxygen contaminants is still relatively low.

When HF dip was done after flashing, re-oxidation had decreased as seen from decrease in 103.5 eV oxide feature. There is minor suboxide, SiO_x, growth based on the small Si 2p shoulder at 101 eV. Also, the oxygen signal is smaller compared to flashed sample but the amount of carbon is much higher after wet chemistry treatment. When looking at the surface structure with STM and LEED, crystallization due to flashing is observed: STM image in Fig. 2a shows clear terrace structure with Si–Si dimer rows running in orthogonal directions on the adjacent terraces (example lines between dark vacancy rows highlighted with the white circles), while LEED shows $(2 \times 1) + (1 \times 2)$ reconstruction, which are common indicators of crystalline surface. After air exposure, terraces are still visible in STM as Fig. 2b suggests, but the surface roughness has increased and the contrast between terraces has dimmed. At the same time, the LEED pattern has reduced to (1×1), meaning that the reconstruction on the surface has been lost. Close-up STM image reveals white dots surrounded by clean surface. Based on the amount of carbon seen in XPS, these dots are concluded to be contaminants from oxygen and carbon on the surface.

Results show that the HF dip after flash significantly decreases the surface from re-oxidizing, and also protects the crystalline structure formed during flash to some extent, although it increases the amount of carbon contamination. A core-level shift can be seen in O 1s spectra between reference sample and treated samples, which means change in bonding environment. The oxygen atoms at the surface are not bonded to Si as they are in native oxide, which is why the peaks shift towards lower binding energy [19]. There is also a possibility of bonding with carbon atoms and a presence of molecular oxygen at the surface. Based on this we conclude, that the treatment provides semi-crystalline surface with no uniform silicon oxide layer before metal deposition, although there is heavy amount of carbon present coming from wet chemistry. This is also the case with n^+-Si.

While for n-Si flash heating proved to be a potential treatment, the situation was different for n^+-Si. Fig. 3 shows how the position of the Fermi level has changed in the band gap of n^+-Si due to flash heating. Prior to flash heating the Fermi level is close to conduction band minimum (CBM), as, expected, but after the heating it shifts closer to the valence band maximum (VBM). Even though the Fermi level position in the gap would suggest the surface to be p-type, it cannot be due to used dopant material. Ex-situ XPS measurement show that samples treated only with HF have observable P on the surface, while in flash heated samples this is not visible (see Supplementary Fig. S2). As the band gap stays relatively same, we conclude that the change in Fermi level position is due to band bending: heating at 1200 °C causes phosphorus atoms to diffuse out from the surface, decreasing the surface concentration. As initially highly doped surface loses dopant atoms while there is more doping under the surface, an n-n^+-Si pair is formed. This causes the band bending shown on the right in Fig. 3.

3.2. Electrical results

Table 1 shows how the contact resistivity was altered with different treatments for low-doped n-Si. All treatments decreased the resistivity significantly compared to out-of-the-box (OotB) reference without any treatments. This is reasonable since the OotB surface has a native oxide and other contaminants, and the surface doping concentration is not too high. Interestingly, there is no difference in contact resistivity between RCA treated and only HF dipped samples. Initially the RCA could be assumed to be better, since it is more thorough cleaning method while HF dip only removes the native oxide. On the other hand, removal

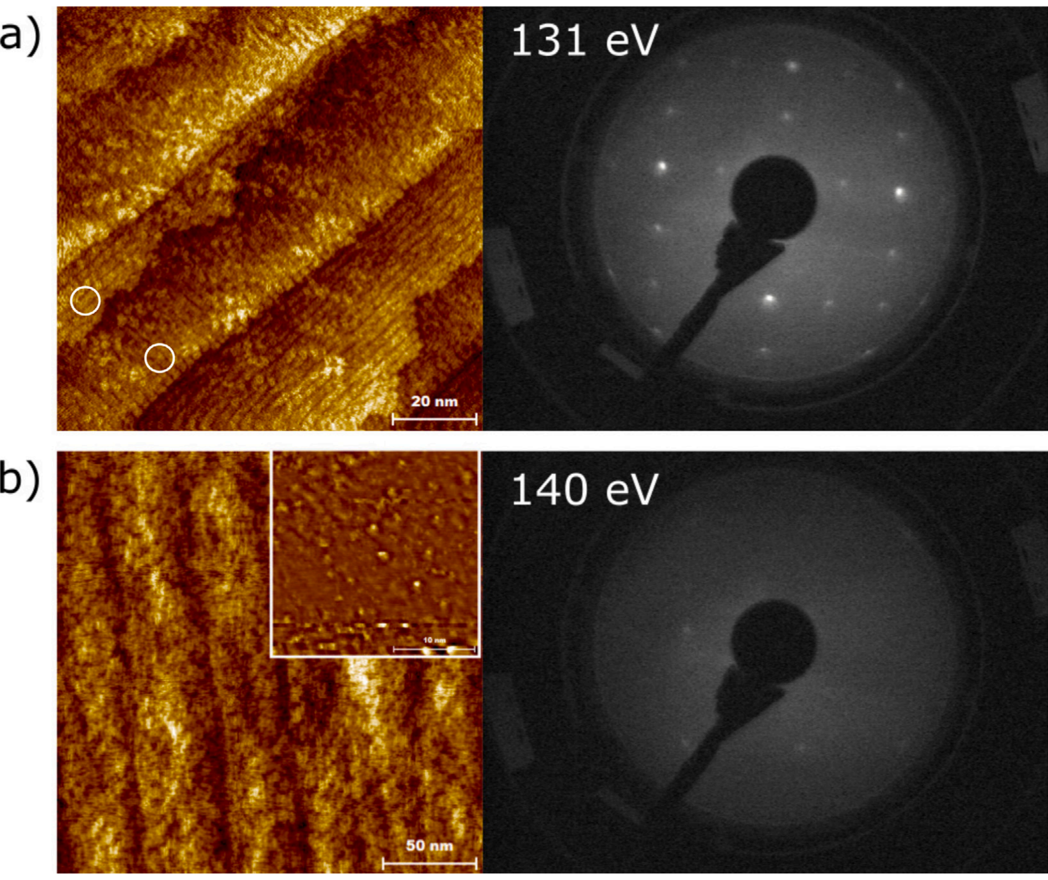

Fig. 2. STM and LEED from n-Si (a) after flash heating, (b) after flash heating followed by HF dip and 23 min of air exposure. Clear terraces with Si–Si dimer rows next to dark lines rising from dimer vacancies originating from to dimer formation (highlighted by white circles) and (2 × 1) + (1 × 2) reconstruction are seen in (a), which degrades to dim terrace structure and (1 × 1) structure seen in (b). We however can see clean surface in STM close-up image in (b) around white dots of carbon and oxygen contaminants.

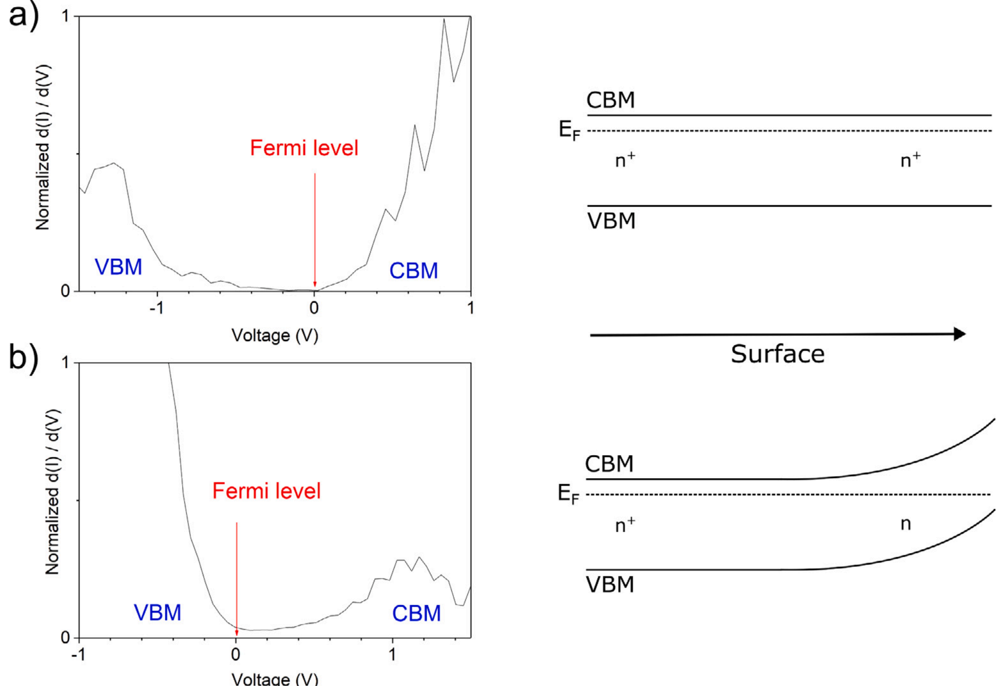

Fig. 3. STS from HF-cleaned n^+-Si (a) before and (b) after flash heating. Fermi level appears to be close to VBM after flash heating, which is due to surface doping concentration decrease induced band bending. Dopant atoms diffuse out from the surface during flash heating, making the surface less doped than the material beneath it, creating an n-n^+-Si pair.

Table 1
Contact resistivity values with n-Si as deposited and after post heating in 350 °C using Pt contacts. Error presented with 95.44% confidence interval.

Treatment	As-deposited [Ω cm^2]	Post-annealed [Ω cm^2]
Out-of-the-box	2.2E3 ± 1.0E3	–
RCA+HF dip (no DIW after HF)	1.5E−1 ± 2.7E−2	–
HF dip	1.5E−1 ± 8.1E−2	1.4E−1 ± 5.4E−3
Flash heating	2.7E−1 ± 3.1E−1	1.3E−1 ± 2.6E−1
Flash heating + HF dip	2.0E−2 ± 2.1E−2	6.7E−2 ± 3.0E−3

Table 2
Contact resistivity values for n$^+$-Si as deposited and after post heating in 350 °C using Ni contacts. Error presented with 95.44% confidence interval.

Treatment	As-deposited [Ω cm^2]	Post-annealed [Ω cm^2]
Out-of-the-box	1.3E−2 ± 5.2E−3	4.6E−2 ± 2.3E−3
HF dip	6.2E−3 ± 1.5E−3	6.1E−3 ± 1.8E−3
Flash heating + HF dip	3.3E−2 ± 2.4E−2	1.0E−2 ± 5.7E−3
5 min 800 °C + HF dip	7.5E−3 ± 2.2E−3	5.6E−3 ± 1.1E−3
HF dip (no DIW) + 5 min 800 °C + HF dip	1.0E−2 ± 3.3E−3	8.9E−3 ± 4.3E−3
HF dip (no DIW) + 30 min 400 °C	7.0E−3 ± 2.6E−3	6.4E−3 ± 6.4E−4
HF dip (no DIW) + 30 min 400 °C + HF dip	4.9E−3 ± 1.6E−3	1.5E−3 ± 6.0E−4
HF dip (lift-off)	7.4E−3 ± 2.2E−3	7.9E−3 ± 3.3E−3

of the native oxide has to remove most of the surface contaminants, because they are on top of the oxide layer. It is also worth noting, that the wafer can have a chemically grown protective oxide on the surface by the manufacturer, thus having less contaminants other than one at the very top of the surface.

Flash heating provided a bit higher contact resistivity compared to HF dip, but still a clear improvement to OotB. While the results from flash and chemical cleaning are in the same order of magnitude, the resulted surfaces after treatments are very different: flash heating provides a clean and crystalline surface with reconstruction, whereas HF dip only removes the native oxide but does not crystallize the surface or create a reconstruction. The downside, which also explains the difference between flash and HF treatments, is that after flashed sample leaves the UHV system, the surface starts to re-oxidize.

The combination of flash heating and HF dip decreased the contact resistivity by five times compared to standalone HF dip or flash heating. As discussed in the surface characterization section, after air exposure the traces of crystalline structure were still visible on the sample with flash heating followed by HF dip. We suggest that the combination of relatively oxygen free and somewhat crystalline surface are behind the resistivity decrease. Absence of full oxide layer enables direct bonding between contact metal and smooth Si terrace without an insulating SiO_2 layer. Crystallinity of the Si surface increases surface uniformity and reduces the number of defects in the interface. Contact resistivity is decreased by post-deposition annealing in flash heated and flash heated + HF dipped samples, but what exactly happens in the interface needs more research.

For the highly doped n$^+$-Si the situation is different compared to lowly doped n-Si. Table 2 shows that combination of flash heating and HF dip in fact increases the contact resistivity compared to OotB reference, whereas HF dip alone reduced the contact resistivity to half compared to the OotB reference value. The reason for this is that the doping concentration in the n$^+$-Si is significantly higher than in n-Si. This enables a formation of ohmic contact even without any surface cleaning, but imposes a threat for a dopant in- and out-diffusion from the surface at high temperatures [21,22]. During flash heating the temperature is 1200 °C, which due to diffusion leads to a significant decrease in dopant concentration, thus degrading the contact resistivity. In n$^+$-Si both Pt and Ni were used as contacts, but no difference between them was observed.

In order to avoid significant dopant atom diffusion from the surface of n$^+$-Si, we decreased the UHV heating temperatures. Already by lowering the heating temperature to 800 °C the contact resistivity decreased in n$^+$-Si. Surprisingly first UHV heating and then dipping into HF provided lower resistivity than HF dip followed by UHV heating, which was still followed by HF dip. The best recipe for decreasing contact resistivity we found for n$^+$-Si was HF dip followed by 30-min heating at 400 °C followed by HF dip. Reason for 400 °C heating to be better than 800 °C most likely is the same as why flash heating did not work as initially was expected: some dopant atom diffusion away from the surface happens already at 800 °C, which however is not as violent compared to flash heating that it would result poorer resistivity as OotB reference.

After the electrical measurements were conducted, metal signal between contacts were detected from multiple samples with ex-situ XPS. We also note that metal silicides were not observed between the contacts while using EDS but were detected when measured with XPS. Based on the Si 2p line shapes both semiconductor substrates had formed silicides with metals, which was confirmed with an exemplarily peak fitting of Si 2p spectrum from post-annealed Pt covered surface seen in Fig. 4. This raised a suspicion of current flowing among some conductive silicide channel on the surface. To investigate this issue, HF dipped samples using both low and high doped substrates were prepared using lift-off lithography. Pt contacts on the low doped silicon were in fact Schottky type. However, Ni contacts on high doped silicon were still Ohmic with similar contact resistivities, and no metal was observed between contacts.

4. Discussion

Resulted Schottky contacts on low doped silicon using lift-off proved that observed contact resistivities on these samples prepared using standard lithography are, in fact, values based on a conductive silicide channel on top of the sample surface, which has formed already prior to any post heating. Despite this, the resulted resistivity is still dependent on how the surface is treated and can be altered. The change in resistivity after post heating is most likely due to smoothing effect of proper UHV heating on Si surface and changes in silicide structure [23]. Based on this, silicide surface channel forms easily at Si surfaces even at low temperature ($<$200 °C) which can make contact resistivity analysis difficult when using standard lithography. Additionally, the silicide component is very strong compared to the bulk 2p components. Heating with the metal also causes formation of silicon oxide, despite the oxide free surface before the metal deposition: Fig. 1 top right corner shows that no oxide peak is visible even after flash heating, HF dip and air exposure. However, after metal deposition and post heating there is a very clear silicon oxide component visible in Fig. 4, even though the surface composition before metallization resembles the spectrum seen in the top right corner of Fig. 1 due to a similar HF treatment and air exposure. Previously, this has been shown to occur when Pt covered

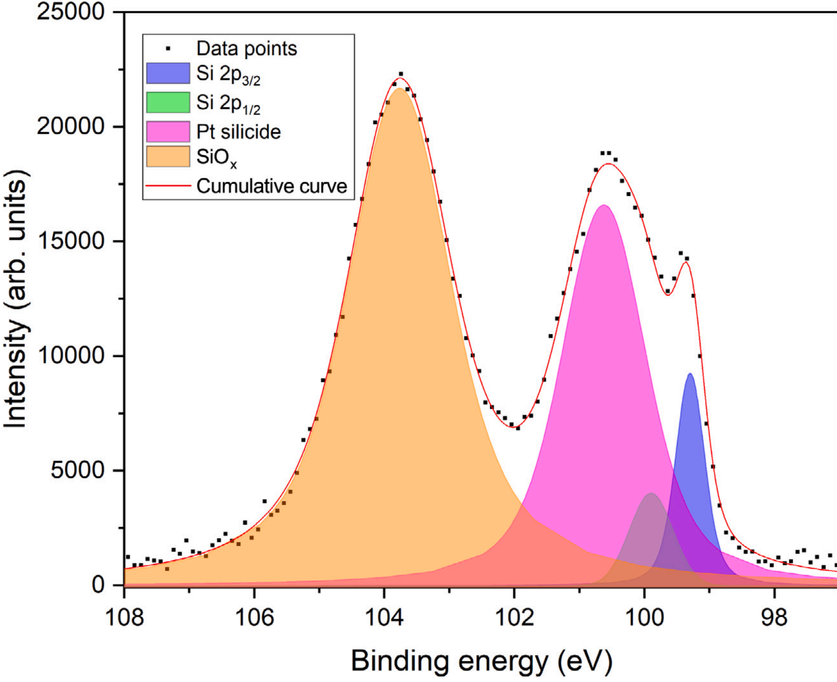

Fig. 4. Fitted Si 2p XPS spectrum from post-annealed Pt covered, HF treated surface, showing a clear additional, metal induced component (purple) rising from platinum silicide. SiO_2 type oxide component intensity is clearly larger than in air-exposed surfaces without metal, indicating Pt-catalyzed oxidation of Si.

silicon has been heated in oxygen background [24]. Even though our heating environment is UHV, the sample has been transported through air and the surface has oxygen. This is most likely the source of oxide for silicon oxidation in our heated silicide samples.

On high doped silicon the contact stayed ohmic despite the change in lithography and the resistivity relatively same. When the surface doping concentration is high enough on Si surface, the effect of silicide surface channel decreases, i.e., current transport is through silicon itself. However, the similarity in resistivity values of flash + HF treated samples indicate that the surface properties of n- and n^+-Si must be similar. Treatment process for both substrates was the same so the surface structure and chemical composition has to be the same. The only difference that these substrates have is the initial doping concentration, however the similar contact resistivity implies similar doping concentration as well, pointing to dopant out-diffusion in n^+-Si.

Phosphorus diffusion has been shown to heavily increase when heating temperature increases, and it can also diffuse out from the surface [21,25]. At the same time, like mentioned in Section 3.1, the P signal was obtained from only HF treated sample, but in flash heated sample the phosphorus signal had disappeared. This indicates that the dopant concentration at the surface of high doped silicon has decreased as a result of heating and, in fact, reached a similar level than in the low doped silicon. This is in line with STS results in Fig. 3. This would also mean that the current would flow along the silicide on surface in flashed n^+-Si rather than in the semiconductor itself.

Dopant out-diffusion on low doped silicon is also possible, but there is indication that the out-diffusion intensity is dependent on the initial doping concentration [21]. As there is roughly four orders of magnitude difference between n- and n^+-Si doping levels, diffusion impacts n^+-Si more, which is why there is much larger difference in flash and HF treated sample results using n^+-Si than n-Si. Similar results with n-Si between flash and HF treatment could imply similar doping concentration on the surface, but we cannot exclude the diffusion. Our previous capacitance-voltage measurements not directly related to this investigation suggest that there is some phosphorus diffusion (see Supplementary Fig. S3). The reason for decreased contact resistivity provided by the combination of flash heating and HF for n-Si is the crystalline surface which is then H terminated. Even though the surface is not perfectly crystalline after 23 min, it is sufficient to provide better contact. Most likely if the doping concentration on n^+-Si could be maintained and a crystalline surface could be produced, the combination of flash and HF would decrease the contact resistivity on that as well.

Already lowering the heating temperature to 800 °C improved contact resistivity on n^+-Si. Still the difference in results between only HF dipped and combination of 800 °C heating and HF dip is in favor for only HF dip, suggesting that there clearly still is P diffusion. This is also supported by literature [22]. HF dip done prior to 800 °C heating seems to increase the contact resistivity, even though surface reconstruction could suggest the opposite: after the heating there is a clear (2 × 1) + (1 × 2) reconstruction seen in the LEED whereas without HF before 800 °C heating there is no LEED pattern visible (see Supplementary Fig. S4). Main difference between surfaces before heating is the native oxide: after HF dip there is no thick oxide layer. Lack of the oxide layer could make the dopant atom out-diffusion easier, which in turn would increase the contact resistivity despite the better surface ordering (i.e., two compensating effects). When the native oxide is on the surface, dopant atoms would not diffuse so easily out from the surface.

The best cleaning recipe found here for n^+-Si was a combination of HF dip and 30-min heating in UHV at 400 °C followed by another HF dip. Oxide removal before heating proved to be better than heating first to 400 °C and then doing HF dip. Oxide free surface probably has been more prone to change of surface properties due to heating. There has been indication that in 350 °C phosphorus starts to diffuse closer to the surface [26]. Here the temperature is a bit higher, but the improvement compared to 800 °C heating or sole HF dip would indicate surface property improvement. Recently it has also been shown that even 400 °C heating in UHV can increase the crystallinity of Si surface and decrease the amount of C contamination [3]. Since the resistivity is lower than in HF treated sample, we conclude that the current path is through actual semiconductor rather than surface silicide between the contacts.

In all samples except n^+-Si OotB and both only HF dipped samples the contact resistivity lowered after the post heating in 350 °C. With platinum, the silicide composition changes from Pt_2Si to PtSi when heating in 350 °C [27]. For Ni, annealing at over 300 °C but under 550

°C has been shown to change Ni_2Si silicide to NiSi, which has lower resistivity [15]. We conclude this change in silicide phase to be the reason for lowered contact resistivity after post heating.

5. Conclusions

We have shown that using proper combination of UHV heating and chemical treatment one can achieve lower contact resistivity than using only traditional wet chemical cleaning (e.g. RCA). Our results indicate how important it is to protect the surface after UHV heating before metal deposition. The hydrogen termination provided by HF after the UHV heating is an important step, and the termination effect holds relatively well even after 23 min.

According to our experiments, a challenge with the UHV heating is changes in the surface doping concentration in particular with high concentrations of surface doping. The UHV flash heating at 1200 °C removes a large amount of phosphorus dopant atoms, and even at 800 °C the phosphorus diffusion is high enough to degrade the contact resistivity for n^+-Si. This diffusion effect was not clearly visible in the lowly doped n-Si, however we suspect some diffusion happening in there as well based on our previous capacitance-voltage measurements (see Supplementary Fig. S3). This makes tailoring the heating temperature and time to suit different samples with different doping concentrations important. For Ni/n^+-Si contacts, we found that the following combination: HF dip followed by 400 °C heating in UHV followed by HF dip decreases the contact resistivity four times as compared to the pure HF dip cleaning, which is probably due to decreasing surface point defects during the UHV heating.

Pt and Ni were found to form silicides with silicon surface even at low temperatures (<200 °C), causing problematic effects which needs to be taken into account when using standard lithography. However, with high enough doping concentration, the current flow was through the semiconductor rather than from the unintentional silicide, i.e., it transported where it should. This underlines the importance of sufficiently high doping concentration when using standard lithography rather than lift-off. Interestingly, even with current being transported through the silicide, the measured resistivity could be altered using the Si surface pretreatments. Mechanisms regarding this need more research.

CRediT authorship contribution statement

Mikko Miettinen: Writing – original draft, Validation, Methodology, Investigation. **Esa Vuorinen:** Writing – review & editing, Methodology, Investigation, Conceptualization. **Juha-Pekka Lehtiö:** Writing – review & editing, Validation. **Zahra Jahanshah Rad:** Writing – review & editing, Validation. **Risto Punkkinen:** Writing – review & editing, Validation. **Mikhail Kuzmin:** Writing – review & editing, Validation. **Jarno Järvinen:** Writing – review & editing, Methodology. **Ville Vähänissi:** Writing – review & editing, Validation. **Pekka Laukkanen:** Writing – review & editing, Validation, Supervision, Funding acquisition, Conceptualization. **Hele Savin:** Writing – review & editing, Validation, Funding acquisition. **Kalevi Kokko:** Writing – review & editing, Supervision.

Declaration of competing interest

The authors declare the following financial interests/personal relationships which may be considered as potential competing interests: Pekka Laukkanen reports financial support was provided by Research Council of Finland. Hele Savin reports financial support was provided by Research Council of Finland. If there are other authors, they declare that they have no known competing financial interests or personal relationships that could have appeared to influence the work reported in this paper.

Acknowledgments

Research Council of Finland and University of Turku Graduate School UTUGS are acknowledged for financial support. Jenny & Antti Wihuri Foundation is acknowledged for providing lithography equipment.

Appendix A. Supplementary data

Supplementary material related to this article can be found online at https://doi.org/10.1016/j.apsusc.2025.162790.

Data availability

Data will be made available on request.

References

[1] F. Bechstedt, Principles of Surface Physics, in: Advanced Texts in Physics, Springer, Berlin, ISBN: 3-540-00635-4, 2003.

[2] Y.J. Chabal, A. Zunger, R.M. Osgood, R. Hull, H. Sakaki (Eds.), Fundamental Aspects of Silicon Oxidation, in: Springer Series in Materials Science, Vol. 46, Springer Berlin Heidelberg, Berlin, Heidelberg, 2001, http://dx.doi.org/10.1007/978-3-642-56711-7.

[3] Z.J. Rad, J.P. Lehtiö, I. Mack, K. Rosta, K. Chen, V. Vähänissi, M. Punkkinen, R. Punkkinen, H.P. Hedman, A. Pavlov, M. Kuzmin, H. Savin, P. Laukkanen, K. Kokko, Decreasing interface defect densities via silicon oxide passivation at temperatures below 450 ° C, ACS Appl. Mater. Interfaces (ISSN: 19448252) 12 (41) (2020) 46933–46941, http://dx.doi.org/10.1021/acsami.0c12636, Publisher: American Chemical Society.

[4] P. Laukkanen, M.P. Punkkinen, M. Kuzmin, K. Kokko, J. L˚ ang, R.M. Wallace, Passivation of III-V surfaces with crystalline oxidation, Appl. Phys. Rev. (ISSN: 19319401) 8 (1) (2021) http://dx.doi.org/10.1063/1.5126629, Publisher: American Institute of Physics Inc..

[5] T. Yamasaki, C. Kaneta, T. Uchiyama, T. Uda, K. Terakura, Geometric and electronic structures of SiO2/Si(001)interfaces, Phys. Rev. B - Condens. Matter Mater. Phys. (ISSN: 1550235X) 63 (11) (2001) http://dx.doi.org/10.1103/PhysRevB.63.115314.

[6] P.K. Hurley, K. Cherkaoui, A. Groenland, Electrically active interface defects in the (100)Si/SiO_x/\chHfO2/TiN system: Origin, instabilities and passivation, ECS Trans. (ISSN: 1938-5862) 3 (3) (2006) 97–110, http://dx.doi.org/10.1149/1.2355702, ISBN: 1566775035 Publisher: The Electrochemical Society Inc.

[7] L. Lin, J. Robertson, Defect states at III-V semiconductor oxide interfaces, Appl. Phys. Lett. (ISSN: 00036951) 98 (8) (2011) 082903–082903–3, http://dx.doi.org/10.1063/1.3556619, Publisher: American Institute of Physics.

[8] M.A. Juntunen, J. Heinonen, V. Vähänissi, P. Repo, D. Valluru, H. Savin, Near-unity quantum efficiency of broadband black silicon photodiodes with an induced junction, Nat. Photonics (ISSN: 17494893) 10 (12) (2016) 777–781, http://dx.doi.org/10.1038/nphoton.2016.226, Place: London Publisher: Nature Publishing Group.

[9] M.A. Leilaeioun, W. Weigand, M. Boccard, Z.J. Yu, K. Fisher, Z.C. Holman, Contact resistivity of the p-Type amorphous silicon hole contact in silicon heterojunction solar cells, IEEE J. Photovolt. (ISSN: 21563403) 10 (1) (2020) 54–62, http://dx.doi.org/10.1109/JPHOTOV.2019.2949430, Publisher: IEEE.

[10] T.G. Allen, J. Bullock, Q. Jeangros, C. Samundsett, Y. Wan, J. Cui, A.c. Hessler-Wyser, S. De Wolf, A. Javey, A. Cuevas, A low resistance calcium/reduced titania passivated contact for high efficiency crystalline silicon solar cells, Adv. Energy Mater. (ISSN: 16146840) 7 (12) (2017) 1–7, http://dx.doi.org/10.1002/aenm.201602606.

[11] S.C. Teng, Z.Y. Liang, C.P. Chou, Y.H. Tsai, P.W. Chiu, Y.H. Wu, Co silicide with low contact resistivity formed by atomic layer deposited cobalt and subsequent annealing, IEEE Electron Device Lett. (ISSN: 15580563) 41 (1) (2020) 139–142, http://dx.doi.org/10.1109/LED.2019.2952921, Publisher: IEEE.

[12] J. Cho, M. Debucquoy, M. Recaman Payo, S. Malik, M. Filipič, H.S. Radhakrishnan, T. Bearda, I. Gordon, J. Szlufcik, J. Poortmans, Contact resistivity reduction on lowly-doped n-type Si using a low workfunction metal and a thin TiO_x interfacial layer for doping-free Si solar cells, Energy Procedia (ISSN: 18766102) 124 (2017) 842–850, http://dx.doi.org/10.1016/j.egypro.2017.09.356.

[13] T. Morimoto, T. Ohguro, H.S. Momose, T. Iinuma, I. Kunishima, K. Suguro, I. Katakabe, H. Nakajima, M. Tsuchiaki, M. Ono, Y. Katsumata, H. Iwai, Self-aligned nickel-mono-silicide technology for high-speed deep submicrometer logic CMOS ULSI, IEEE Trans. Electron Devices (ISSN: 15579646) 42 (5) (1995) 915–922, http://dx.doi.org/10.1109/16.381988.

[14] C. Lavoie, F.M. D'Heurle, C. Detavernier, C. Cabral, Towards implementation of a nickel silicide process for CMOS technologies, in: Microelectronic Engineering, Vol. 70, 2003, pp. 144–157, http://dx.doi.org/10.1016/S0167-9317(03)00380-0, ISSN: 01679317 Issue: 2-4.

[15] J. Foggiato, W.S. Yoo, M. Ouaknine, T. Murakami, T. Fukada, Optimizing the formation of nickel suicide, in: Materials Science and Engineering B: Solid-State Materials for Advanced Technology, Vol. 114–115, 2004, pp. 56–60, http://dx.doi.org/10.1016/j.mseb.2004.07.033, ISSN: 09215107 Issue: SPEC. ISS.

[16] B. Imbert, R. Pantel, S. Zoll, M. Gregoire, R. Beneyton, S. del Medico, O. Thomas, Nickel silicide encroachment formation and characterization, Microelectron. Eng. (ISSN: 01679317) 87 (3) (2010) 245–248, http://dx.doi.org/10.1016/j.mee.2009.06.003, Publisher: Elsevier B.V..

[17] T. Pasanen, V. Vähänissi, N. Theut, H. Savin, Surface passivation of black silicon phosphorus emitters with atomic layer deposited \chSiO2/\chAl2O3 stacks, Energy Procedia (ISSN: 18766102) 124 (2017) 307–312, http://dx.doi.org/10.1016/j.egypro.2017.09.304, Publisher: Elsevier B.V..

[18] The Relationship Between Resistivity and Dopant Density for Phosphorus-and Boron-Doped Silicon, Vol. 400–464, Commerce Department, National Instute of Standards and Technology (NIST), 1981, Backup Publisher: Commerce Department, National Instute of Standards and Technology (NIST).

[19] J.F. Moulder, W.F. Stickle, P.E. Sobol, K.D. Domben, Handbook of X-ray Photoelectron Spectroscopy, Perkin-Elmer Corporation, ISBN: 978-0-470-01422-6, 1992, http://dx.doi.org/10.1002/0470014229.ch22.

[20] D.K. Schroder, Semiconductor Material and Device Characterization, first ed., Wiley, 2005, http://dx.doi.org/10.1002/0471749095.

[21] S.P. Murarka, Phosphorus out-diffusion during high temperature anneal of phosphorus-doped polycrystalline silicon and \chSiO2, J. Appl. Phys. (ISSN: 00218979) 56 (8) (1984) 2225–2230, http://dx.doi.org/10.1063/1.334281.

[22] Y. Sato, K. Imai, N. Yabumoto, Phosphorus pileup and sublimation at the silicon surface, J. Electrochem. Soc. (ISSN: 0013-4651) 144 (7) (1997) http://dx.doi.org/10.1149/1.1837853.

[23] C.A. Chang, Ptsi contact metallurgy: Comparison of different annealing sequences, annealing time and ambients, and deposition techniques of Pt, 1986, http://dx.doi.org/10.1063/1.336888, ISSN: 00218979 Issue: 9 Pages: 3116–3121 Publication Title: Journal of Applied Physics Volume: 59.

[24] H. Kobayashi, T. Yuasa, K. Yamanaka, K. Yoneda, Y. Todokoro, Mechanism of platinum-enhanced oxidation of silicon at low temperatures, J. Chem. Phys. (ISSN: 0021-9606) 109 (12) (1998) 4997–5001, http://dx.doi.org/10.1063/1.477112.

[25] J.S. Christensen, A.Y. Kuznetsov, H.H. Radamson, B.G. Svensson, Phosphorus diffusion in silicon; Influence of annealing conditions, in: Materials Research Society Symposium - Proceedings, Vol. 669, 2001, http://dx.doi.org/10.1557/proc-669-j3.9, ISSN: 02729172.

[26] S. Zaima, O. Nakatsuka, A. Sakai, J. Murota, Y. Yasuda, Interfacial reaction and electrical properties in Ni/Si and Ni/SiGe(C) contacts, Appl. Surf. Sci. (ISSN: 01694332) 224 (1–4) (2004) 215–221, http://dx.doi.org/10.1016/j.apsusc.2003.08.049.

[27] S. Morgan, R. Williams, J. Mooney, An XPS study of thin Pt and Ir silicide overlayer formation on Si(100)2 X 1 surfaces, Appl. Surf. Sci. (ISSN: 0169-4332) 56–58 (1992) 493–500, http://dx.doi.org/10.1016/0169-4332(92)90277-5.